Accepted Manuscript

Bioactive heterocycles containing a 3,4,5-trimethoxyphenyl fragment exerting potent antiproliferative activity through microtubule destabilization

Dong-Jun Fu, Jia-Jia Yang, Ping Li, Yu-Hui Hou, Sheng-Nan Huang, Matthew Alexander Tippin, Victor Pham, Liankun Song, Xiaolin Zi, Wei-Li Xue, Li-Rong Zhang, Sai-Yang Zhang

PII: S0223-5234(18)30625-1

DOI: 10.1016/j.ejmech.2018.07.060

Reference: EJMECH 10595

To appear in: *European Journal of Medicinal Chemistry*

Received Date: 28 April 2018

Revised Date: 25 July 2018

Accepted Date: 25 July 2018

Please cite this article as: D.-J. Fu, J.-J. Yang, P. Li, Y.-H. Hou, S.-N. Huang, M.A. Tippin, V. Pham, L. Song, X. Zi, W.-L. Xue, L.-R. Zhang, S.-Y. Zhang, Bioactive heterocycles containing a 3,4,5-trimethoxyphenyl fragment exerting potent antiproliferative activity through microtubule destabilization, *European Journal of Medicinal Chemistry* (2018), doi: 10.1016/j.ejmech.2018.07.060.

Graphic abstract

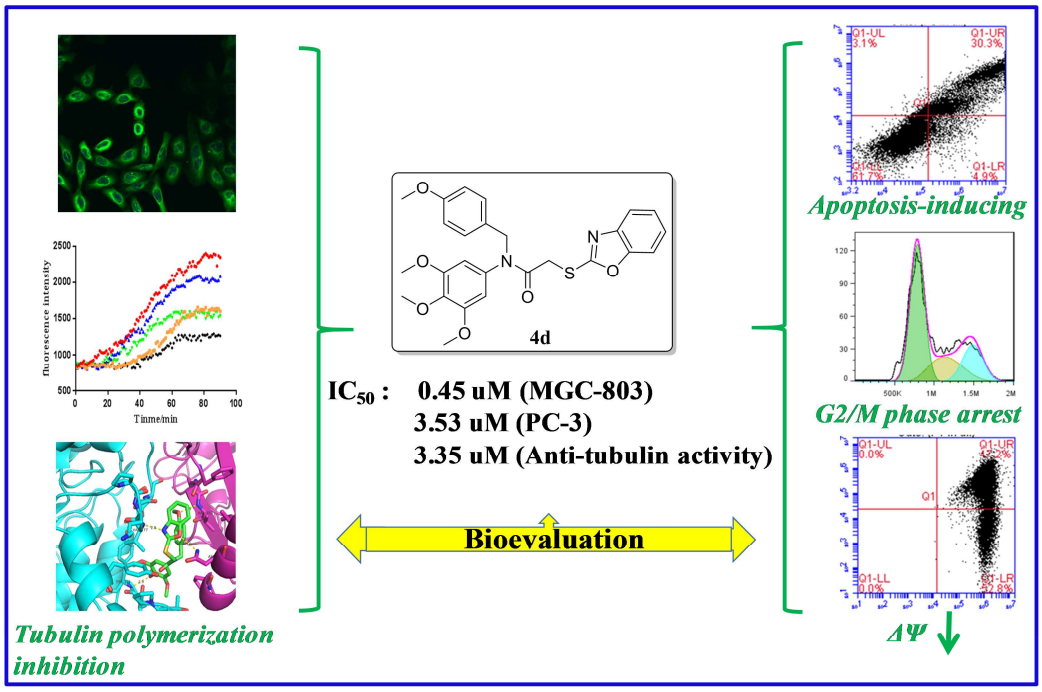

Bioactive heterocycles containing a 3,4,5-trimethoxyphenyl fragment exerting potent antiproliferative activity through microtubule destabilization

Dong-Jun Fu[a], Jia-Jia Yang[a], Ping Li[a], Yu-Hui Hou[a], Sheng-Nan Huang[a], Matthew Alexander Tippin[b], Victor Pham[b], Liankun Song[b], Xiaolin Zi[b], Wei-Li Xue[c], Li-Rong Zhang[d,*] and Sai-Yang Zhang[d,*]

[a]School of Pharmaceutical Sciences & Collaborative Innovation Center of New Drug Research and Safety Evaluation, Zhengzhou University, Zhengzhou 450001, China

[b]Department of Urology, University of California, Irvine, Orange, CA 92868, USA

[c]The first affiliated hospital of zhengzhou university, Zhengzhou University, Zhengzhou 450052, China

[d]School of Basic Medicine, Zhengzhou university, Zhengzhou 450001, China

*Corresponding author, E-mail addresses: Zhnaglirongzzu@126.com (L.-Y. Zhang) and celeron16@163.com (S.-Y. Zhang)

Abstract

Novel bioactive heterocycles containing a 3,4,5-trimethoxyphenyl fragment as antiproliferative agents by targeting tubulin were synthesized and their preliminary structure activity relationships (*SARs*) were explored. Among all these chemical agents, 2-(Benzo[d]oxazol-2-ylthio)-*N*-(4-methoxybenzyl)-*N*-(3,4,5-trimethoxyphenyl)acetamide (**4d**) exhibited the potent antiproliferative activity against MGC-803 cells with an IC_{50} value of 0.45 uM by induction of G2/M pahse arrest and cell apoptosis. In addition, **4d** could change the membrane potential ($\Delta\Psi$) of the mitochondria against MGC-803 cells. Importantly, **4d** acted as a novel tubulin polymerization inhibitor binding to colchicine site with an IC_{50} value of 3.35 uM.

Keywords

3,4,5-trimethoxyphenyl fragment; G2/M; Apoptosis; ΔΨ; Tubulin polymerization; Colchicine site

1. Introduction

Disrupting tubulin system is a well-verified method for the development of highly efficient antitumor candidate drugs because microtubules play a key role in the essential cellular processes including the movement of organelles and the maintenance of cell shape [1]. Tubulin targeting agents with anticancer activity are known to interact with tubulin through at least four binding sites: the laulimalide site, paclitaxel site, vinblastine site, and colchicine site [2]. Many natural products and chemical molecules (**Fig.1**) binding to the colchicine site display excellent anticancer activity by microtubule destabilization [3-5]. However, the potential clinical applications of many colchicine site tubulin inhibitors have so far been halted by the significant toxicities, low

solubility, and their low bioavailibility [6]. Therefore, it is very necessary to design and synthesis novel colchicine site tubulin inhibitors for cancer therapy.

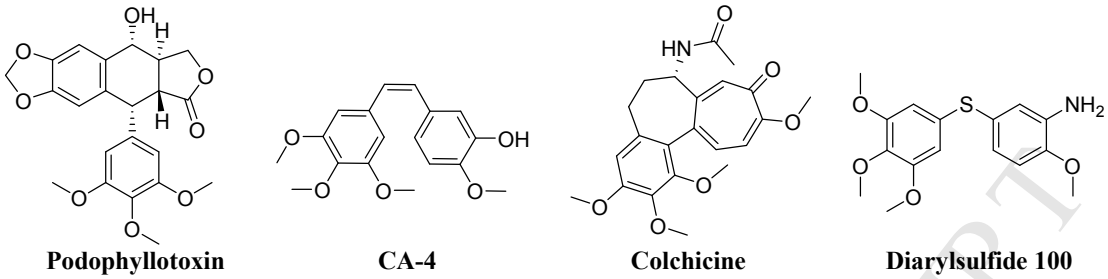

Fig.1. Recently developed colchicine site tubulin inhibitors

Recently, a variety of colchicine site tubulin inhibitors were designed, synthesized and evaluated their biological mechanisms [7]. As shown in **Fig. 2**, synthetic molecules such as phenstatin, BCN-105P and CP-461 are acknowledged to play potent anticancer activity by engaging tubulin on colchicine site [8]. These molecules lead to cancer cells death by interfering with the polymerization of tubulin and arresting cancer cells in the G2/M phase [9]. Based on chemical structures of these colchicine site tubulin inhibitors (phenstatin, BCN-105P and CP-461 in **Fig 2**), the 3,4,5-trimethoxyphenyl unit is a crucial fragment to induce microtubule depolymerisation [10].

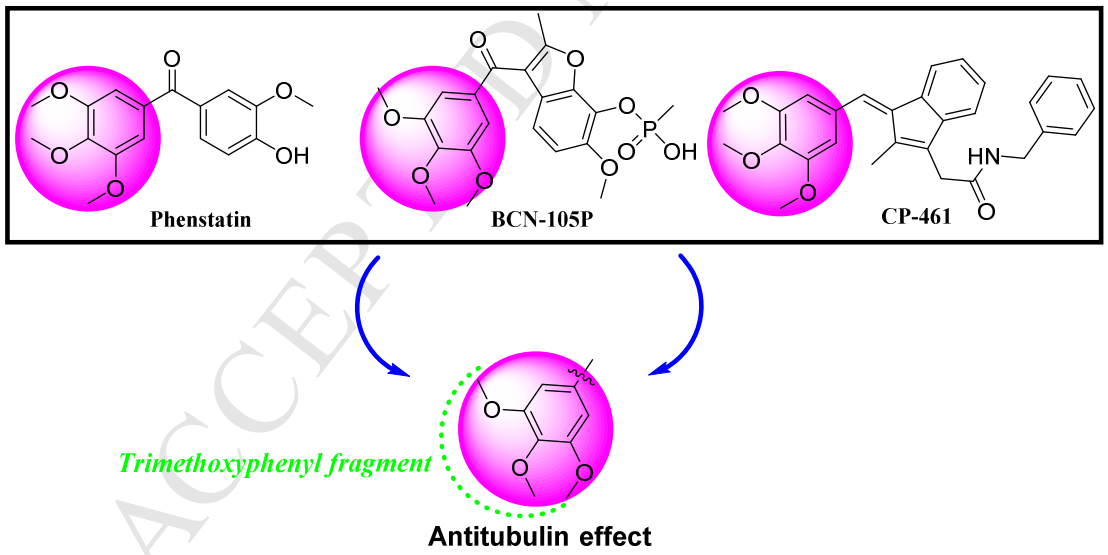

Fig.2. 3,4,5-Trimethoxyphenyl derivatives as colchicine site tubulin inhibitors

On the other hand, several well-known bioactive heterocycle scaffolds, such as pyridine, 1,3,4-thiadiazole, 1*H*-benzo[d]imidazole, 3-methyl-3H-pyrazole and benzo[d]oxazole, displayed potent antiproliferative activity or antitubulin activity [11-14]. In addition, We have reported two series of tubulin inhibitors: (1) *β*-lactam-azide

analogues as colchicine site tubulin polymerization inhibitors effectively inhibited MGC-803 xenograft tumor growth without causing significant loss of body weight [15, 16]; (2) 4-methyl-*N*-((1-(3-phenoxybenzyl)-1*H*-1,2,3-triazol-4-yl)methyl)benzene sulfonamides could significantly inhibit tubulin polymerization with an IC_{50} of 2.41 μM [17]. To discovery more potent tubulin polymerization inhibitors or anticancer agents [18-27], we designed and synthesized a variety of bioactive heterocycles containing the antitubulin trimethoxyphenyl fragment in this paper. As shown in **Fig. 3**, this rational design might help us gain an insight into the structural requirements for the discovery of potent colchicine site tubulin inhibitors.

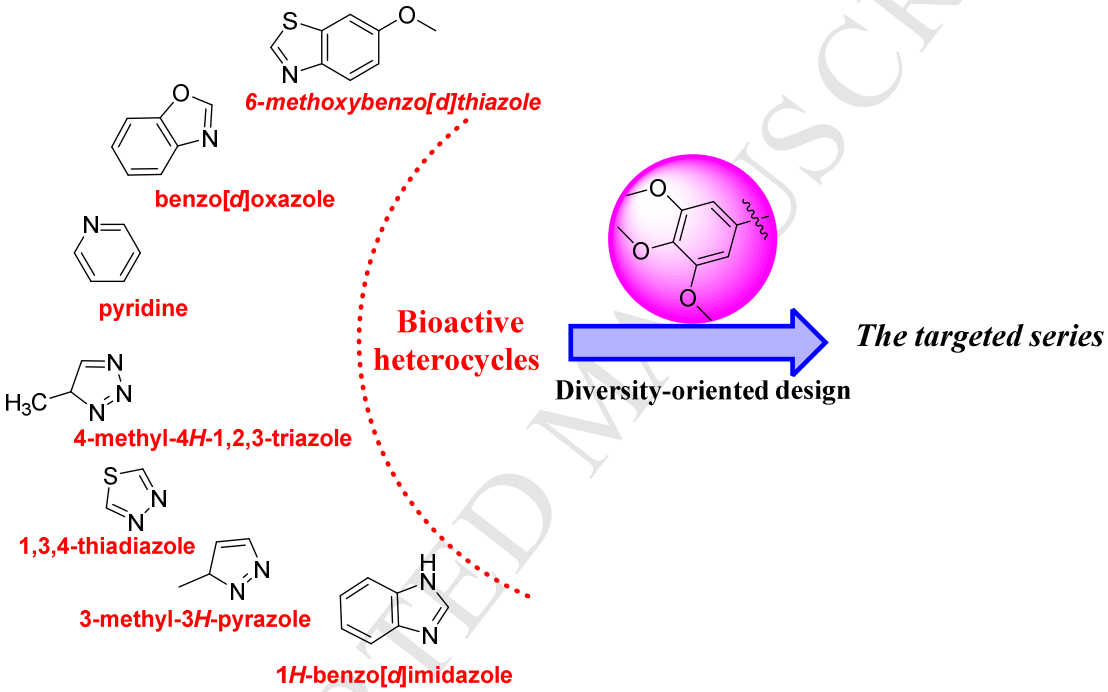

Fig.3. The diversity-oriented design of heterocycles containing a 3,4,5-trimethoxyphenyl fragment in this work

2. Results and discussion

2.1. Chemistry

The synthetic route of bioactive heterocycles containing a 3,4,5-trimethoxyphenyl fragment were shown in **Scheme 1**. 3,4,5-Ttrimethoxyaniline **1** was subjected to nucleophilic substitution reaction with 1-(chloromethyl)-4-methoxybenzene to afford 3,4,5-trimethoxy-*N*-(4-methoxybenzyl)aniline **2** in the presence of appropriate base. The intermediate **2** was reacted with different acyl chloride to obtain the amide analogues **3a~3d** in the dichloromethane solvent system. The target analogues **4a~4j** were easily obtained at the reflux condition with different sulfhydryl heterocycles.

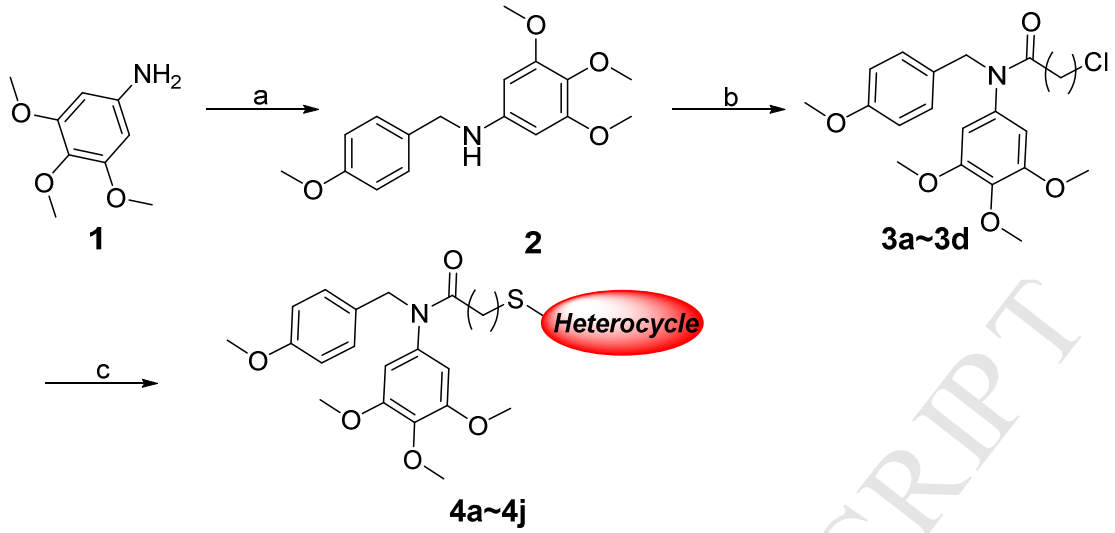

Scheme 1. Reagents and conditions: (a) K_2CO3, 4-methoxybenzyl chloride, acetone, reflux; (b) Acyl chloride derivatives, dichloromethane, rt, 78-85 % yield; (c) NaOH, thio-heterocyclic derivatives, acetone, reflux.

2.2. Antiproliferative activity

In order to discovery novel colchicine site tubulin inhibitors and potent anticancer agents, we evaluated the anticancer activity in vitro of all bioactive heterocycles containing a 3,4,5-trimethoxyphenyl fragment **4a~4j** against several cancer cell lines (PC-3, MGC-803 and EC-109) using the MTT assay. In this paper, colchicine as an well-known colchicine site tubulin inhibitor was used as the reference drug in the MTT assay [28].

Table 1. Antiproliferative activity of the synthetic derivatives **4a~4j**

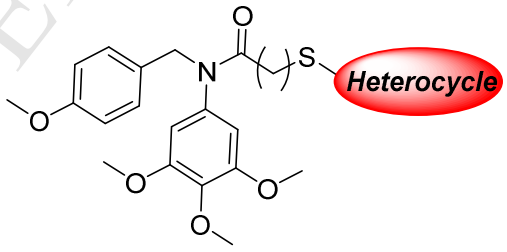

Compound	Heterocycle	n[a]	IC_{50} (μM)[b]		
			MGC-803	PC-3	EC-109
4a	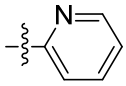	1	2.41±0.27	7.51±0.33	15.95±4.47
4b	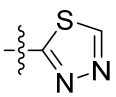	1	1.15±0.18	5.53±1.21	9.84±0.12

4c	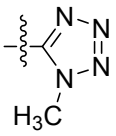	1	2.49±0.15	10.54±1.67	5.54±0.17
4d	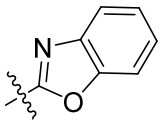	1	0.45±0.12	3.53±0.01	24.75±2.74
4e	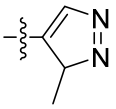	1	2.96±0.08	44.95±3.45	>80
4f	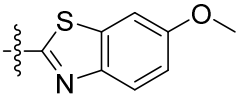	1	1.27±0.11	20.21±2.25	>80
4g	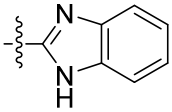	1	1.23±0.32	14.35±3.35	42.62±0.9
4h	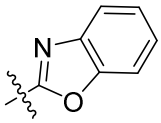	2	0.64±0.01	20.20±0.36	12.61±0.76
4i	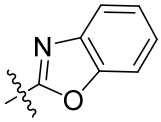	3	1.29±0.01	32.67±1.12	10.97±0.76
4j	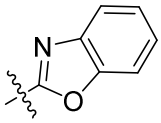	4	1.36±0.11	45.63±1.02	7.65±0.64
Colchicine	---	---	0.177±0.01	0.13±0.01	1.24±0.15

[a]"n" represents the number of -CH_2-.
[b]Antiproliferative activity was assayed by exposure for 48 h.

The anticancer activity in vitro results against all three cancer cells for the candidate compounds **4a~4j** were shown in **Table 1**. All these chemical compounds **4a~4j** exhibited the effective activity against MGC-803 cells. Particularly, 2-(Benzo[d]oxazol-2-ylthio)-*N*-(4-methoxybenzyl)-*N*-(3,4,5-trimethoxyphenyl)acetamide (**4d**) showed the most excellent antiproliferative activity with an IC_{50} value of 0.45 μM against MGC-803 cancer cells. These antiproliferative activity results indicate that bioactive heterocycles containing a 3,4,5-trimethoxyphenyl fragment display potent anticancer activity in vitro and could be used as the leading compounds to explore their detailed antiproliferative mechanisms.

To explore the effect of heterocycle for the inhibitory activity, different bioactive heterocycles including pyridine, 1,3,4-thiadiazole, 1-methyl-1*H*-tetrazole, benzo[d]oxazole, 3-methyl-3*H*-pyrazole, 6-methoxybenzo[d]thiazole, 1*H*-benzo[d]imidazole, benzo[d]oxazole,

benzo[d]oxazole, and benzo[d]oxazole were introduced into the targeted compounds. Replacing the 1-methyl-1*H*-tetrazole scaffold of **4c** with 3-methyl-3*H*-pyrazole ring (**4e**) led to a decrease of the anticancer activity in vitro against the EC-109 cells. However, changing the 6-methoxybenzo[d]thiazole ring of **4f** to 1,3,4-thiadiazole ring of **4b** led to a significant improvement of the activity against MGC-803, PC-3 and EC-109 cell lines. These inhibitory results indicate that heterocycles of compounds **4a~4j** exhibited the important effect for the anticancer activity in vitro.

Because of the potent antiproliferative activity for **4d** with a benzo[d]oxazole scaffold, more benzo[d]oxazole derivatives with different length of carbon linkers were designed, synthesized and evaluated their antiproliferative activity. With the extension of carbon linker length by one carbon, two carbon, and three carbon, the antiproliferative activity was decreased (**4d *vs* 4h or 4i or 4j**) against MGC-803 and PC-3 cells. These results suggested that the linker between benzo[d]oxazole and 3,4,5-trimethoxyphenyl ring plays a significant role in their activities.

*2.3. compound **4d** induced apoptosis*

Based on the antiproliferative activity results above, 2-(Benzo[d]oxazol-2-ylthio)-*N*-(4-methoxybenzyl)-*N*-(3,4,5-trimethoxyphenyl)acetamide (**4d**) was chosen to do apoptosis assays to investigate whether **4d** could induce apoptosis against MGC-803 cells (**Fig. 4**). After treatment with different concentrations of **4d** (0, 200nM, 400nM and 600nM) for 48 h, the percentage of apoptotic cells was changed obviously from the control group. Especially, the apoptotic rate at 600nM treatment was 35.2%, which is obviously higher than the apoptotic rate without any treatment. These results in **Fig. 4** illustrated that compound **4d** could induce apoptosis against MGC-803 cells.

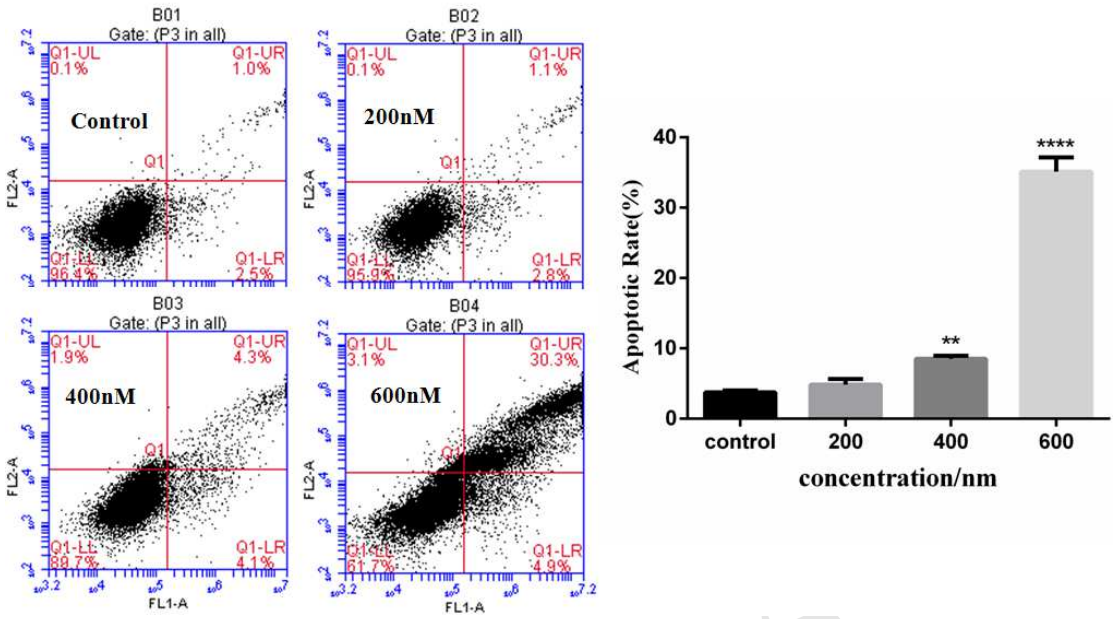

Fig. 4. Compound **4d** could induce apoptosis of MGC-803 cells after treatment 48h. **: $p < 0.01$ versus control, ****: $p < 0.0001$ versus control.

*2.4. compound **4d** regulated apoptosis-related proteins*

Apoptosis as a physiological form of programmed cell death is very necessary for tissue homeostasis by elimination of harmful cells [29]. It is often correlated with the deregulation of the Bcl-2 family proteins that control the intrinsic pathway of apoptosis [30, 31]. Based on the apoptosis results in **Fig. 4**, we further investigated the expression of apoptosis-related proteins (Bcl-2, PARP, and XIAP). As shown in **Fig. 5**, the protein levels of PARP, Bcl-2, and XIAP were decreased in concentration-dependent manners after treatment of compound **4d** (0, 200nM, 400nM and 600nM). However, the expresion level of cleaved-PARP was increased. The westernblot assay on apoptosis-related proteins illustrated that targeted compound **4d** was a potential apoptosis inducer.

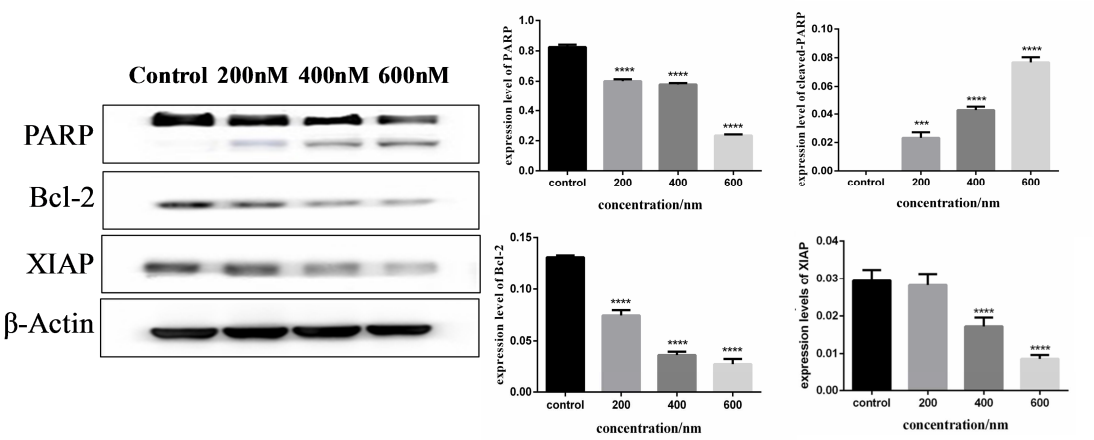

Fig. 5. The expression of Bcl-2, PARP, XIAP, and *β*-Actin was examined by western blot analysis. MGC-803 cells were incubated with compound **4d** (0, 200nM, 400nM and 600nM) for 48 h. ***: $p < 0.001$ versus control, ****: $p < 0.0001$ versus control.

*2.5. compound **4d** induced G2/M phase cell cycle arrest*

The effects of **4d** on cell cycle phase arrest in MGC-803 cells were also evaluated. After treatment for 48 h with compound **4d** (0, 200nM and 400nM), cells were harvested and analyzed by flow cytometry. As shown in **Fig.6**, compound **4d** can prolong the G2 phase, shorten the S phase and G1 phase compared to the control cells. Especially, compound **4d** at 400 nM increased to 20.71% of G2/M cell cycle distribution. The above results showed that compound **4d** caused cell cycle arrest at G2/M phase in MGC-803 cells.

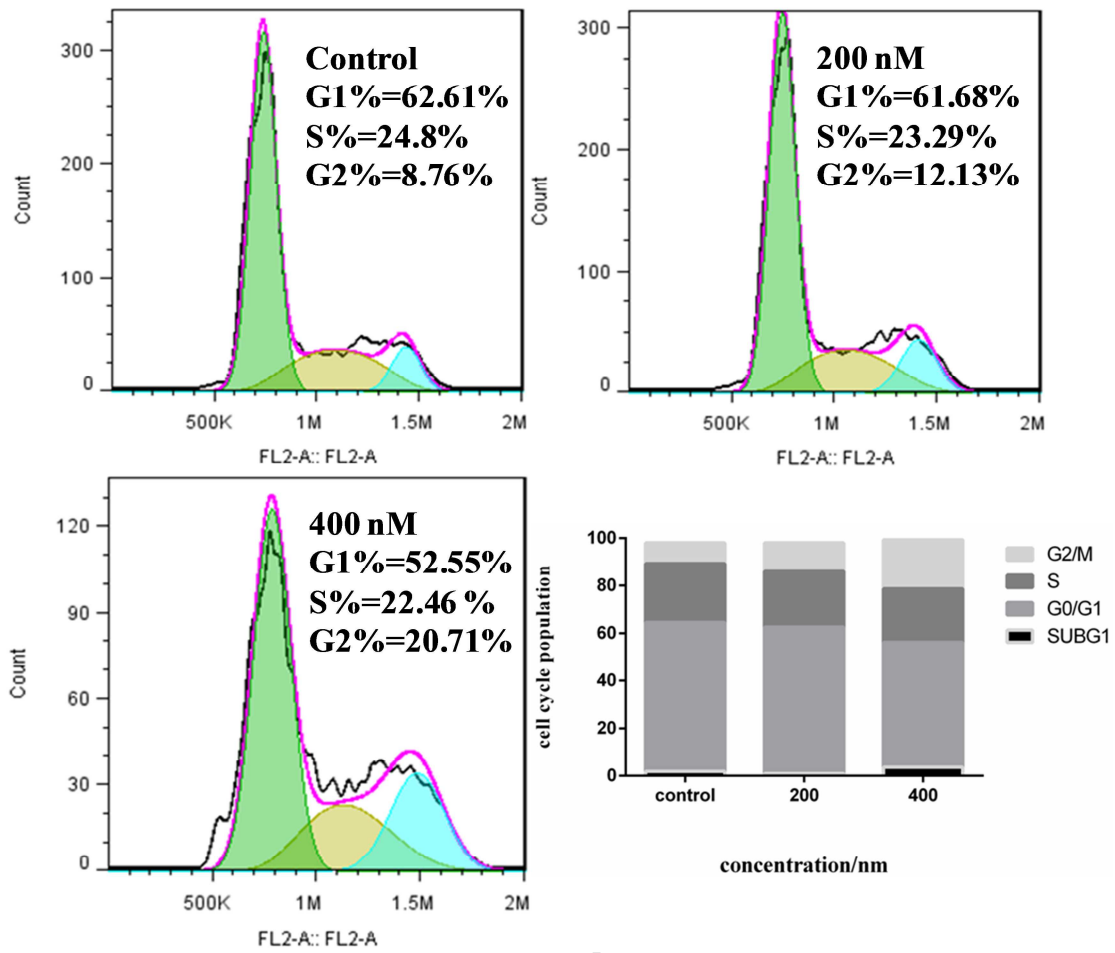

Fig.6. Cell cycle analysis of **4d** (0, 200nM and 400nM) against MGC-803 cells for 48h.

2.6. compound **4d** *regulated cell cycle related proteins*

Cell cycle progress is driven by members of the cyclin-dependent kinase family proteins when bound to their Cyclin partners [32]. CyclinB was purified as the catalytic activity in mitosis promoting factor that upon injection drives interphase cells into mitosis [33]. As shown in **Fig.7**, compound **4d** down regulated cyclin B1 and CDK1 with the increase of concentrations, which lead to cell arrest in G2/M phase.

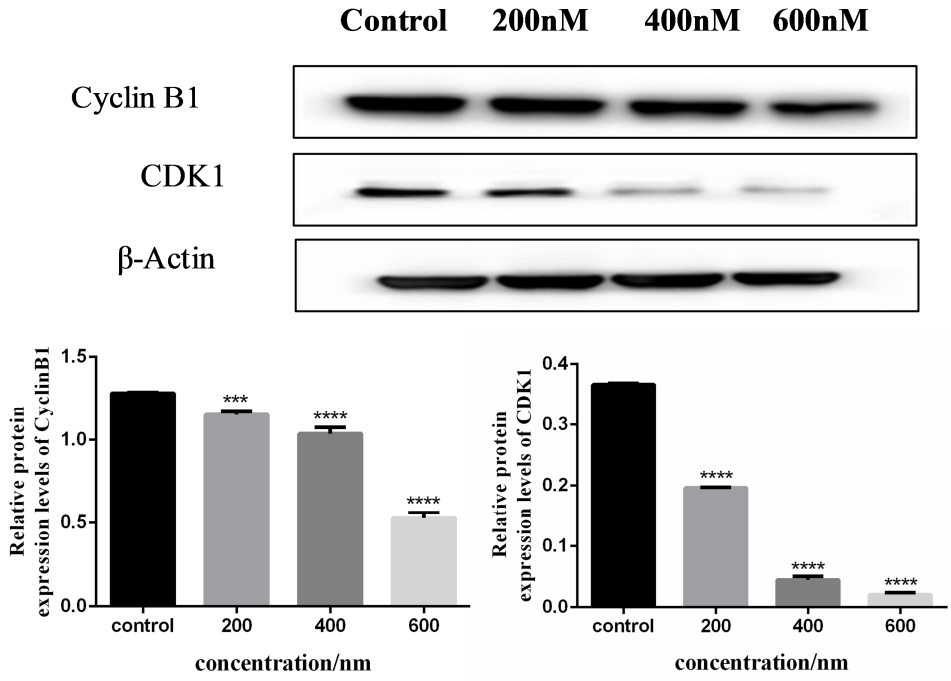

Fig. 7. The expression of cyclin B1, CDK1 and β-actin was examined by western blot analysis against MGC-803 cells for 48 h. ***: $p < 0.001$ versus control, ****: $p < 0.0001$ versus control.

*2.7. compound **4d** changed the membrane potential (ΔΨ) of the mitochondria*

The changes of mitochondrial membrane potential usually associated with the apoptosis [34]. In this work, we also evaluated the change of mitochondrial membrane potential with the treatment of compound **4d**. After MGC-803 cells were incubated with **4d** (0, 200nM, 400nM, 600nM) for 48 h, the mitochondrial membrane potential was decreased in a concentration-dependent manner. As shown in **Fig. 8**, the percentages of cells at 400nM and 600nM were 39.9% and 52.8%, significantly higher than that of the control group (4.4%).

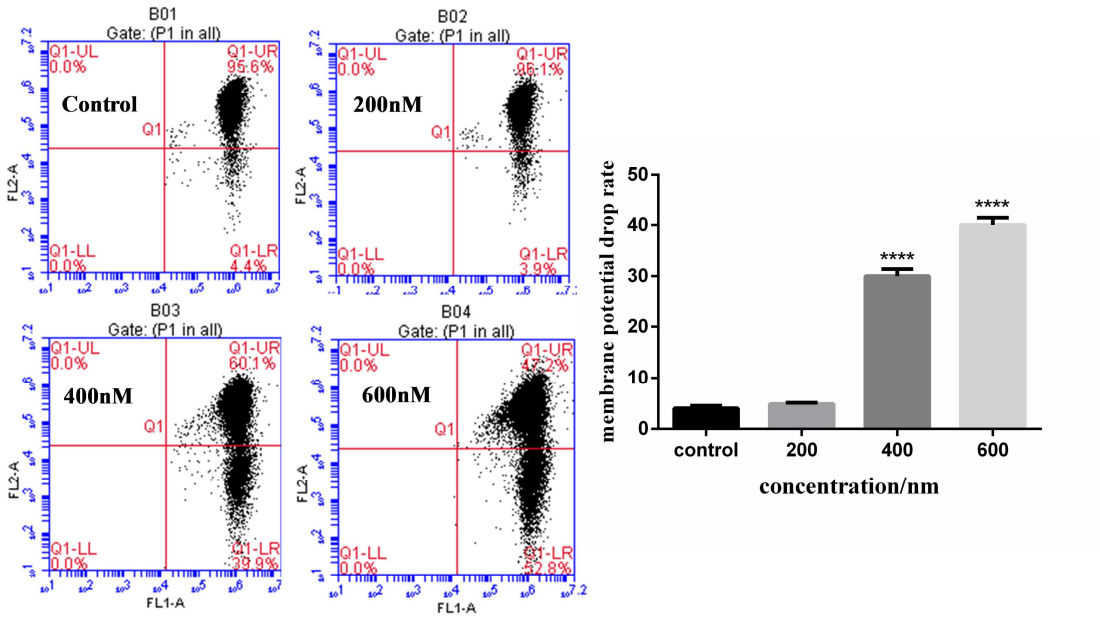

Fig. 8. MGC-803 cells were treated with **4d** (0, 200nM, 400nM, 600nM) for 48 hours. ***: $p < 0.001$ versus control, ****: $p < 0.0001$ versus control.

*2.8. compound **4d** inhibited tubulin polymerization in MGC-803 cells by immunostaining assay*

To explore the effects to tubulin, we selected **4d** as a representative compound in a immunostaining screening. MGC-803 cells were were treated for 0h, 4h and 8h with **4d** (600nM) to examine the effect on microtubules reorganization during the mitosis process. As shown in **Fig. 9**, 4 hours treatment with **4d** (600nM) depolymerized interphase microtubules moderately whereas 8h treatment induced strong depolymerization of interphase microtubules, indicating that **4d** is a potential tubulin polymerization inhibitor (**Fig. 9**).

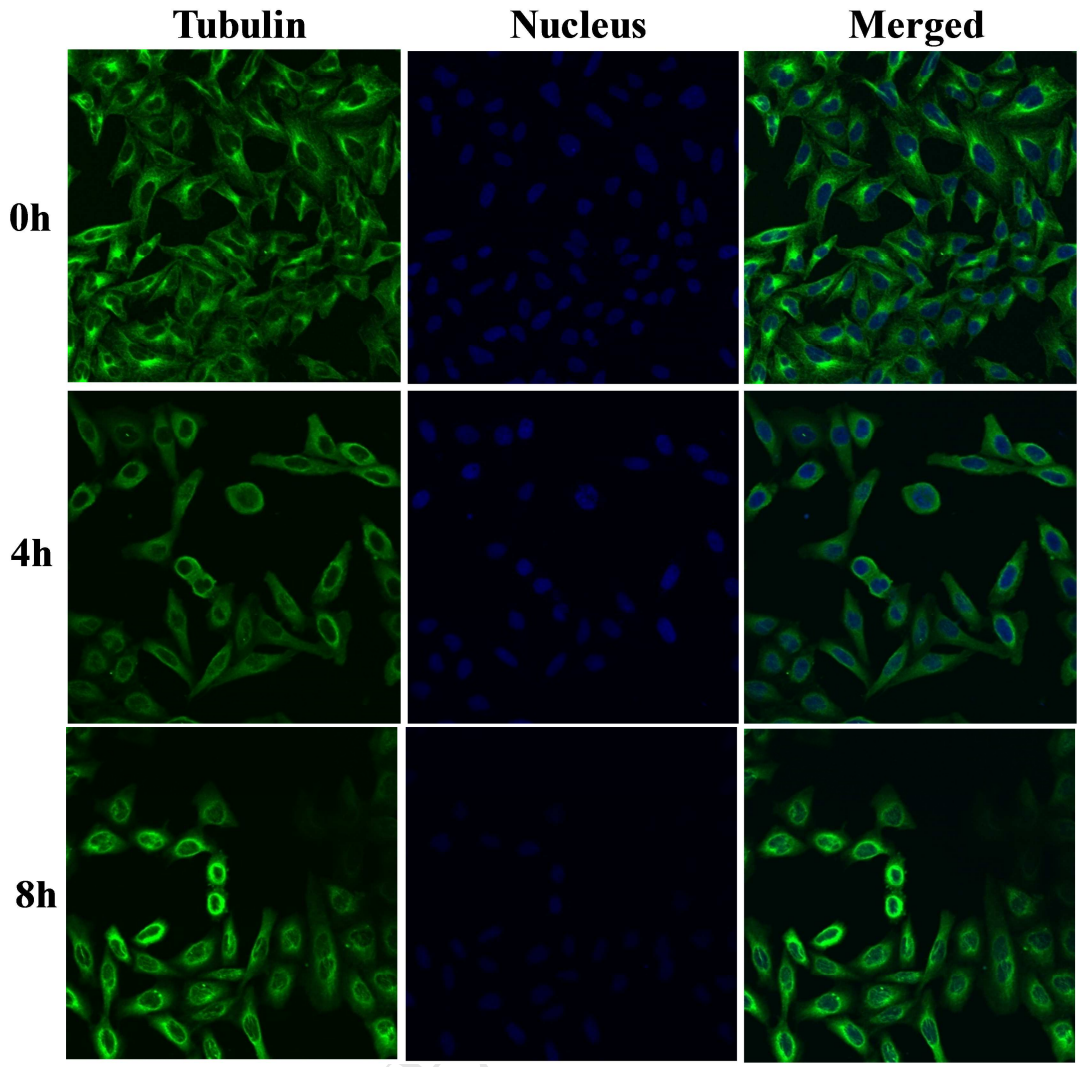

Fig. 9. Compound **4d** showed strong depolymerizing effects on the interphase microtubule network. MGC-803 cells were incubated in the presence of 600 nM of compound **4d** for 0h, 4h and 8h, respectively.

2.9. compound **4d** *displayed potent tubulin polymerization inhibitory activity in vitro*

In addition, the in vitro tubulin polymerization inhibition activity of compound **4d** was evaluated because of its best antiproliferative activity results among target analogues **4a~4j**. When tubulin was incubated with the tested compound **4d** (1uM, 2uM and 4uM), the increased tendency of the fluorescence intensity was obviously slowed down. The IC_{50} value of compound **4d** was 3.35 μM against tubulin (**Fig. 10A**). It revealed **4d** was a novel tubulin polymerization inhibitor.

In order to evaluate whether compound **4d** directly binds to tubulin at the colchicine binding site, we carried out *N*,*N*′-ethylene-bis(iodoacetamide) (EBI) assay in MGC-803 cells according to a previously published paper [35]. Preincubation of

compound **4d** at 400 uM prevented the formation of the EBI: β-tubulin adduct, resulting in the decrease of the adduct band comparing with DMSO and EBI treatment, which was consistent with the effect of colchicine at 5 μM. Thus, the assay (**Fig. 10B**) indicated that compound **4d** directly bind to the cochicine-binding site of β-tubulin.

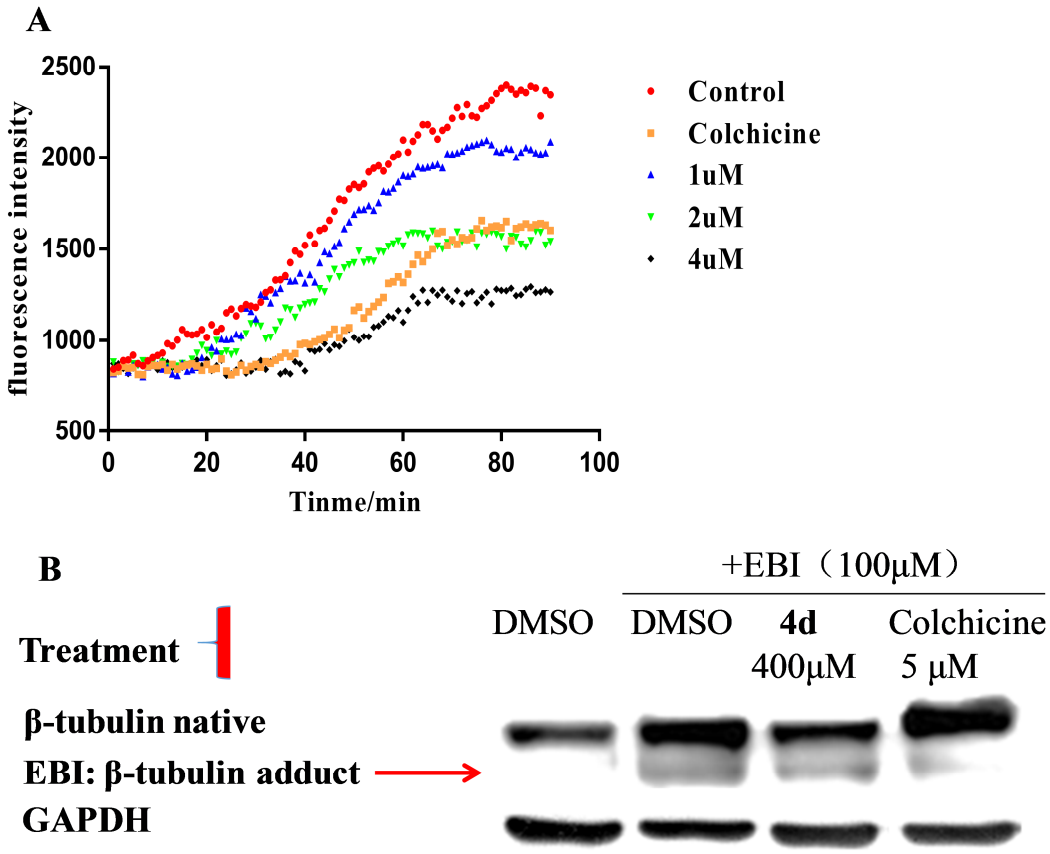

Fig. 10: (A) Tubulin polymerization inhibitory activity of **4d.** (B) EBI competition assay on MGC-803 cells.

*2.10. Molecular Modeling study of compound **4d***

Compound **4d** displayed the potent tubulin polymerization inhibition activity in the screening above, and we then selected it as the optimized compound for the following docking studies. To investigate the binding site of **4d** with tubulin-microtubule system, molecular modeling studies were performed by autodock software (PDB code: 1SA0).

As shown in **Fig.11**, methoxy group of 4-methoxyphenyl ring of compound **4d** formed a hydrogen bond with the residues VAL353. In addition, *p*-methoxy group of 3,4,5-trimethoxyphenyl ring of compound **4d** formed a hydrogen bond with the residues TYR224, indicating the importance of trimethoxyphenyl ring for its potent antiproliferative activity. Importantly, the oxygen atom and nitrogen atom of benzo[*d*]oxazole formed two hydrogen bond with the residues ASN329 and VAL177 respectively. These results explained that the

benzo[*d*]oxazole was better than other heterocycles for the inhibitory effect against MGC-803 cells (**Fig. 11A**). As a reference, colchicine was then docked using the same protocol and compared **4d**. In the **Fig. 11B**, colchicine (wathet blue structure) was docked into a similar pocket as **4d** (pink structure).

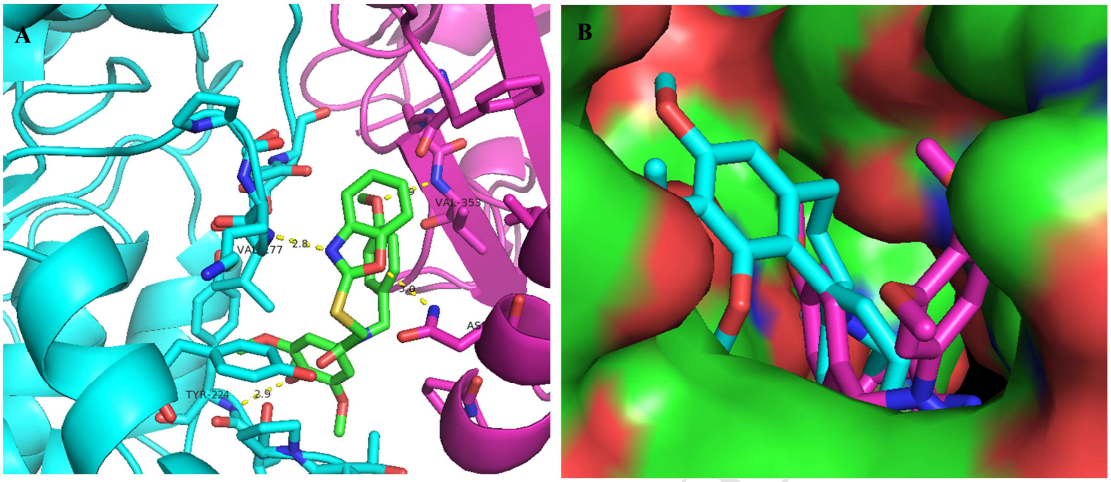

Fig. 11: Molecular docking results of the compound **4d** (PDB code: 1SA0). (A) hydrogen bonds between **4d** and residues. (B) A similar pocket between colchicine and **4d**.

3. Conclusions

Bioactive heterocycles containing a 3,4,5-trimethoxyphenyl ring were designed, synthesized and evaluated for their antiproliferative activities. Among all these analogues, compound **4d** possessed the best antiproliferative ability with an IC_{50} value of 513nM against MGC-803 cells. Preliminary mode of action studies demonstrated that **4d** halted cell cycle progression at the G2/M phase, induced apoptosis and altered the expression of apoptosis-related proteins against MGC-803 cells. The immunofluorescence assays, in vitro tubulin polymerization inhibition experiment, EBI competition assays, and molecular modeling studies identified that compound **4d** was a novel tubulin polymerization inhibitor probably binding to the colchicine site. In summary, compound **4d** could be used as a potential anticancer candidate for further clinical research.

4. Experiment section.

4.1 General

Reagents and solvents were used according to our previous refs [19].

*4.2 General procedure for the synthesis of compounds **2***

To a solution of 3,4,5-trimethoxyaniline **1** (5 mmol) in acetone (20 mL), K_2CO_3 (5 mmol) and 1-(chloromethyl)-4-methoxybenzene (5 mmol) were

added. After the mixture was stirred at 60 °C for 10 h, the reaction extracted with EtOAc and water. The organic layer was washed with aqueous $NaHCO_3$, water, and brine, dried over anhydrous Na_2SO_4, and then concentrated. The residue was purified by column chromatography with petroleum/ethyl acetate (8:1) as an eluent to afford the target compound **2**.

*4.3 General procedure for the synthesis of compounds **4a~4j***

A solution of compound **2** (2 mmol) in dichloromethane was added dropwise to a 2-chloroacetyl chloride, 3-chloropropanoyl chloride, 4-chlorobutanoyl chloride or 5-chloropentanoyl chloride (2 mmol) at 60 °C. After the mixture was stirred for 50 min, the reaction mixture was diluted with water. THF were removed in vacuum, and the residue was taken up by ethyl acetate. The combined organic layer was washed by aqueous $NaHCO_3$, water, and brine, dried over anhydrous Na_2SO_4, and concentrated to provide the crude products **3a~3d** without purification.

Thio-heterocyclic derivatives (5 mmol) was added to the solution of crude products **3a~3d** (5 mmol) in acetone. After stirring at 60 °C for 2 h, the reaction mixture was concentrated to remove then treated with a solution of ethyl acetate (30 mL) and H_2O (30 mL). The organic layer was washed with aqueous Na_2CO_3, water, and brine, dried over anhydrous Na_2SO_4, and then concentrated. The residue was purified by column chromatography with petroleum/ethyl acetate (10:1) as an eluent to afford the target compound **4a~4j**.

*3,4,5-Trimethoxy-N-(4-methoxybenzyl)aniline (**2**)*

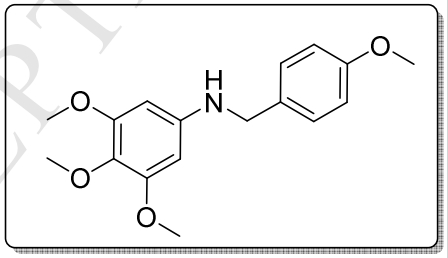

Yield:36%. White solid, m.p.:101~102 ^{o}C. ^{1}H NMR (400 MHz, DMSO) δ 7.30 (d, *J* = 8.4 Hz, 2H), 6.89 (d, *J* = 8.5 Hz, 2H), 6.01 – 5.81 (m, 3H), 4.16 (d, *J* = 5.8 Hz, 2H), 3.73 (s, 3H), 3.65 (s, 6H), 3.51 (s, 3H). ^{13}C NMR (100 MHz, DMSO) δ 158.08, 153.30, 145.39, 132.13, 128.58, 128.56, 113.62, 90.22, 60.09, 55.42, 54.97, 46.37. HRMS (ESI) (m/z) $[M + H]^+$ calcd for $C_{17}H_{22}NO_4$, 304.1549; found, 304.1553.

*N-(4-methoxybenzyl)-2-(pyridin-2-ylthio)-N-(3,4,5-trimethoxyphenyl)acetamide (**4a**)*

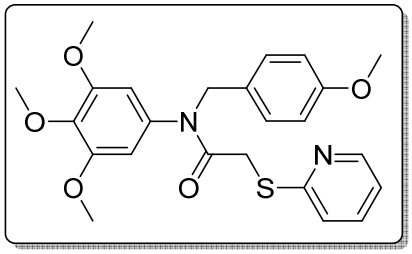

Yield:79%. White solid, m.p.:91~92 °C.^{1}H NMR (400 MHz, $CDCl_3$) δ 8.17 (d, *J* = 4.6 Hz, 1H), 7.37 (td, *J* = 7.9, 1.8 Hz, 1H), 7.15 (d, *J* = 8.1 Hz, 1H), 7.08 (d, *J* = 8.6 Hz, 2H), 6.86 (dd, *J* = 6.7, 5.2 Hz, 1H), 6.71 (d, *J* = 8.6 Hz, 2H), 6.20 (s, 2H), 4.73 (s, 2H), 3.78 (s, 2H), 3.75 (s, 3H), 3.69 (s, 3H), 3.61 (s, 6H). ^{13}C NMR (100 MHz, $CDCl_3$) δ 167.43, 158.00, 156.70, 152.39, 147.93, 136.68, 136.31, 134.94, 129.55, 128.72, 120.96, 118.58, 112.59, 104.93, 59.91, 55.07, 54.25, 51.78, 32.12. HRMS (ESI) (m/z) $[M + H]^+$ calcd for $C_{24}H_{27}N_2O_5S$, 455.1641; found, 455.1648.

*2-((1,3,4-Thiadiazol-2-yl)thio)-N-(4-methoxybenzyl)-N-(3,4,5-trimethoxy phenyl)acetamide (**4b**)*

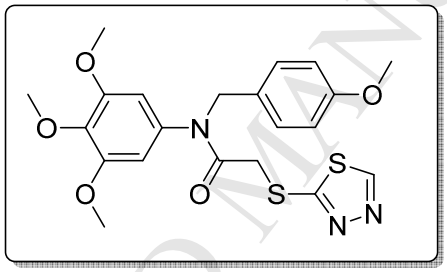

Yield:42%. White solid, m.p.:124~125 °C. ^{1}H NMR (400 MHz, $CDCl_3$) δ 8.91 (s, 1H), 7.07 (d, *J* = 8.6 Hz, 2H), 6.73 (d, *J* = 8.6 Hz, 2H), 6.21 (s, 2H), 4.73 (s, 2H), 4.03 (s, 2H), 3.79 (s, 3H), 3.71 (s, 3H), 3.66 (s, 6H). ^{13}C NMR (100 MHz, $CDCl_3$) δ 165.36, 163.85, 158.16, 152.67, 150.60, 137.04, 135.52, 129.60, 128.13, 112.72, 104.76, 59.93, 55.20, 54.27, 52.14, 36.73. HRMS (ESI) (m/z) $[M + H]^+$ calcd for $C_{21}H_{24}N_3O_5S_2$, 462.1157; found, 462.1162.

*N-(4-Methoxybenzyl)-2-((1-methyl-1H-tetrazol-5-yl)thio)-N-(3,4,5-trimet hoxyphenyl)acetamide (**4c**)*

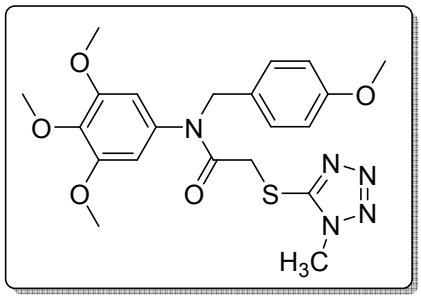

Yield:52%. White solid, m.p.:104~105 °C. ^{1}H NMR (400 MHz, $CDCl_3$) δ 7.04 (d, *J* = 8.6 Hz, 2H), 6.73 (d, *J* = 8.6 Hz, 2H), 6.20 (s, 2H), 4.71 (s, 2H), 3.99 (s, 2H), 3.89 (s, 3H), 3.79 (s, 3H), 3.71 (s, 3H), 3.67 (s, 6H).

^{13}C NMR (100 MHz, $CDCl_3$) δ 164.91, 158.21, 152.75, 152.58, 137.17, 135.23, 129.57, 127.90, 112.75, 104.71, 59.94, 55.23, 54.27, 52.30, 36.59, 32.55. HRMS (ESI) (m/z) $[M + H]^+$ calcd for $C_{21}H_{26}N_5O_5S$, 460.1655; found, 460.1659.

*2-(Benzo[d]oxazol-2-ylthio)-N-(4-methoxybenzyl)-N-(3,4,5-trimethoxyphenyl)acetamide (**4d**)*

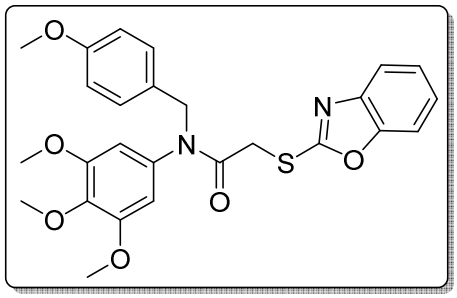

Yield:80%. White solid, m.p.:132~133 °C.^{1}H NMR (400 MHz, $CDCl_3$) δ 7.45 – 7.36 (m, 1H), 7.35 – 7.27 (m, 1H), 7.25 – 7.13 (m, 2H), 7.09 (d, *J* = 8.6 Hz, 2H), 6.72 (d, *J* = 8.6 Hz, 2H), 6.25 (s, 2H), 4.76 (s, 2H), 3.95 (s, 2H), 3.77 (s, 3H), 3.71 (s, 3H), 3.65 (s, 6H). ^{13}C NMR (100 MHz, $CDCl_3$) δ 166.54, 164.18, 159.17, 153.68, 152.00, 141.77, 138.05, 136.74, 130.65, 129.26, 124.29, 123.99, 118.22, 113.73, 110.00, 105.86, 60.97, 56.20, 55.30, 53.14, 36.04. HRMS (ESI) (m/z) $[M + H]^+$ calcd for $C_{26}H_{27}N_2O_6S$, 495.1590; found, 495.1597.

N-(4-methoxybenzyl)-2-((3-methyl-3*H*-pyrazol-4-yl)thio)-*N*-(3,4,5-trimethoxyphenyl)acetamide (**4e**)

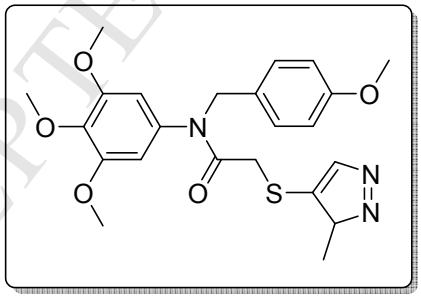

Yield:68%. White solid, m.p.:97~98 °C.^{1}H NMR (400 MHz, $CDCl_3$) δ 7.03 (d, *J* = 8.6 Hz, 2H), 6.93 (s, 1H), 6.85 (s, 1H), 6.72 (d, *J* = 8.6 Hz, 2H), 6.11 (s, 2H), 4.68 (s, 2H), 3.77 (s, 3H), 3.71 (s, 3H), 3.66 (s, 2H), 3.64 (s, 6H), 3.61 (s, 3H). ^{13}C NMR (100 MHz, $CDCl_3$) δ 167.72, 159.07, 153.55, 140.52, 137.86, 136.88, 130.53, 129.39, 129.31, 122.60, 113.64, 105.78, 60.93, 56.16, 55.28, 52.90, 37.71, 33.53. HRMS (ESI) (m/z) $[M + H]^+$ calcd for $C_{23}H_{28}N_3O_5S$, 458.1750; found, 458.1758.

*2-((6-Methoxybenzo[d]thiazol-2-yl)thio)-N-(4-methoxybenzyl)-N-(3,4,5-trimethoxyphenyl)acetamide (**4f**)*

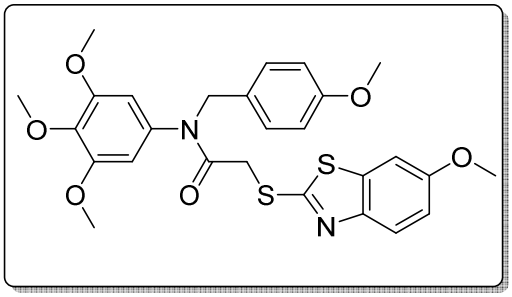

Yield:52%. White solid, m.p.:129~130 °C. ^{1}H NMR (400 MHz, $CDCl_3$) δ 7.50 (d, *J* = 8.9 Hz, 1H), 7.13 (d, *J* = 2.5 Hz, 1H), 7.09 (d, *J* = 8.6 Hz, 2H), 6.90 (dd, *J* = 8.9, 2.5 Hz, 1H), 6.71 (d, *J* = 8.6 Hz, 2H), 6.23 (s, 2H), 4.75 (s, 2H), 3.94 (s, 2H), 3.77 (s, 3H), 3.75 (s, 3H), 3.70 (s, 3H), 3.63 (s, 6H). ^{13}C NMR (100 MHz, $CDCl_3$) δ 165.95, 161.35, 158.08, 156.08, 152.59, 146.41, 136.92, 135.94, 135.89, 129.58, 128.37, 120.77, 113.77, 112.69, 104.82, 103.09, 59.91, 55.17, 54.78, 54.25, 51.97, 35.78. HRMS (ESI) (m/z) $[M + H]^+$ calcd for $C_{27}H_{29}N_2O_6S_2$, 541.1467; found, 541.1469.

*2-((1H-benzo[d]imidazol-2-yl)thio)-N-(4-methoxybenzyl)-N-(3,4,5-trimethoxyphenyl)acetamide (**4g**)*

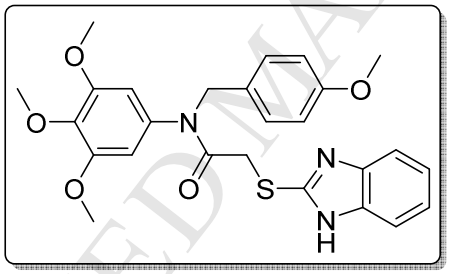

Yield:61%. White solid, m.p.:144~145 °C. ^{1}H NMR (400 MHz, $CDCl_3$) δ 7.45 (s, 2H), 7.16 – 7.01 (m, 4H), 6.73 (d, *J* = 8.6 Hz, 2H), 6.18 (s, 2H), 4.79 (s, 2H), 3.78 (s, 3H), 3.69 (s, 3H), 3.64 (s, 6H), 3.60 (s, 2H). ^{13}C NMR (100 MHz, $CDCl_3$) δ 169.25, 158.29, 152.77, 148.38, 137.12, 135.26, 129.39, 127.56, 121.21, 112.89, 104.45, 59.95, 55.20, 54.26, 52.12, 32.58. HRMS (ESI) (m/z) $[M + H]^+$ calcd for $C_{26}H_{28}N_3O_5S$, 494.1750; found, 494.1758.

*3-(Benzo[d]oxazol-2-ylthio)-N-(4-methoxybenzyl)-N-(3,4,5-trimethoxyphenyl)propanamide (**4h**)*

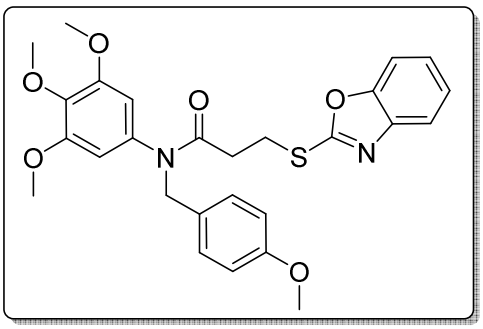

Yield:37%. yellow oil. ^{1}H NMR (400 MHz, $CDCl_3$) δ 7.50 – 7.37 (m, 1H), 7.37 – 7.26 (m, 1H), 7.14 (td, *J* = 7.0, 1.4 Hz, 2H), 7.07 (d, *J* = 8.6 Hz, 2H), 6.73 (d, *J* = 8.6 Hz, 2H), 5.98 (s, 2H), 4.72 (s, 2H), 3.70 (s, 3H), 3.64 (s, 3H), 3.50 (s, 8H), 2.66 (t, *J* = 6.5 Hz, 2H). ^{13}C NMR (100 MHz, DMSO) δ 165.17, 159.66, 153.84, 148.24, 146.50, 136.49, 132.51, 131.82, 125.30, 124.42, 119.04, 118.59, 112.99, 108.47, 104.52, 100.55, 55.60, 50.75, 50.02, 47.19, 28.78, 22.86. HRMS (ESI) (m/z) $[M + H]^+$ calcd for $C_{27}H_{29}N_2O_6S$, 509.1746; found, 509.1748.

*4-(Benzo[d]oxazol-2-ylthio)-N-(4-methoxybenzyl)-N-(3,4,5-trimethoxyphenyl)butanamide (**4i**)*

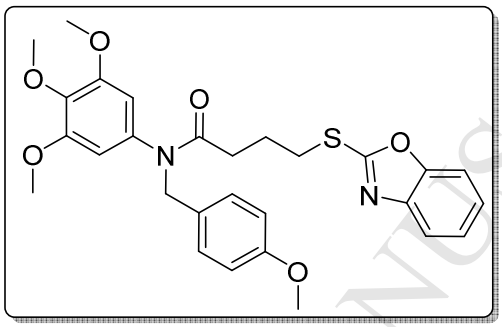

Yield:50%. yellow oil. ^{1}H NMR (400 MHz, $CDCl_3$) δ 7.53 – 7.40 (m, 1H), 7.39 – 7.27 (m, 1H), 7.22 – 7.13 (m, 2H), 7.06 (d, *J* = 8.6 Hz, 2H), 6.72 (d, *J* = 8.6 Hz, 2H), 6.02 (s, 2H), 4.69 (s, 2H), 3.76 (s, 3H), 3.69 (s, 3H), 3.58 (s, 6H), 3.27 (t, *J* = 7.0 Hz, 2H), 2.24 (dd, *J* = 8.9, 5.3 Hz, 2H), 2.09 (t, *J* = 6.9 Hz, 2H). ^{13}C NMR (100 MHz, DMSO) δ 166.21, 159.58, 153.79, 148.30, 146.53, 136.62, 132.50, 132.30, 125.28, 124.67, 119.02, 118.59, 113.06, 108.44, 104.56, 100.56, 55.68, 50.86, 49.99, 47.08, 27.34, 26.46, 19.80. HRMS (ESI) (m/z) $[M + H]^+$ calcd for $C_{28}H_{31}N_2O_6S$, 523.1903; found, 523.1907.

*5-(Benzo[d]oxazol-2-ylthio)-N-(4-methoxybenzyl)-N-(3,4,5-trimethoxyphenyl)pentanamide (**4j**)*

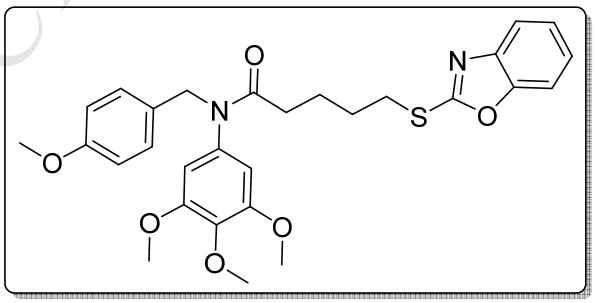

Yield:49%. yellow oil. ^{1}H NMR (400 MHz, $CDCl_3$) δ 7.47 (dd, *J* = 7.6, 0.9 Hz, 1H), 7.38 – 7.28 (m, 1H), 7.22 – 7.10 (m, 2H), 7.04 (t, *J* = 5.7 Hz, 2H), 6.70 (d, *J* = 8.6 Hz, 2H), 6.03 (s, 2H), 4.69 (s, 2H), 3.74 (s, 3H), 3.68 (s, 3H), 3.60 (s, 6H), 3.17 (t, *J* = 6.5 Hz, 2H), 2.09 (d, *J* = 4.8 Hz, 2H), 1.83 – 1.65 (m, 4H).^{13}C NMR (100 MHz, DMSO) δ 166.88, 159.73,

153.76, 148.26, 146.53, 136.65, 132.47 (d, J = 6.2 Hz), 125.24, 124.77, 118.99, 118.55, 113.03, 108.42, 104.56, 100.60, 55.66, 50.89, 49.98, 47.03, 28.29, 26.75, 23.68, 19.31. HRMS (ESI) (m/z) $[M + H]^+$ calcd for $C_{29}H_{33}N_2O_6S$, 537.2059; found, 537.2062.

4.4 Biological experiments

Cell culture, flow cytometry analysis, western blot, immunostaining assay, tubulin polymerization assay in vitro and docking experiments were proceeded according to our reported papers in European journal of medicinal chemistry and Scientific reports [15, 19, 20].

4.5 Measurement of mitochondrial membrane potential (ΔΨ)

1.5×10^5 cells were seeded into 6-well plates per well with RPMI-1640 media, and treated with different concentration of compound **4d** for 48 hours. Then 1 mg/ml JC-1 probe was added to incubate with an equal volume of cell suspension at 37 °C for 15 min to measure cell MMP and rinsed twice with PBS. The signal of retained JC-1 dye was determined by flow cytometry to detect the MMP.

4.6 Molecular modeling Studies

Molecular modeling was performed using the autodock 4 software from the Scripps Research Institute. Molecules were first generated using Pymol software. Following generation, the files were converted to the .pdbqt format using OpenBabel. The drugs were then docked using AutoDockTools from MGLTools via the Scripps institute. The docked conformations and information were then docked and their resulting conformations were visualized using Pymol.

Several steps were used to prepare the protein for docking of the drugs. First, using pymol the magnesium ions were removed. Next, the GDP and GTP molecules were selectively removed from a copy of the protein , generated using the methods described above, and docked back onto 1SA0 to examine the docking accuracy with their sites. The molecules preferentially clustered around their crystallization coordinates, indicating the docking was reasonably calibrated.

Dockings were initially performed using a blind docking method on a lower resolution docking. This was followed by a series of resolving steps to attempt to fine tune the compounds to their preferential binding site. The top twenty-five binding conformations of each blind docking were chosen as areas to designate a new, higher resolution grid box. The binding selection chosen as preferred for each drug are the conformations that are most consistent across the dockings, as well as the most realistic for inhibition.

Acknowledgment

This work was supported by the National Natural Sciences Foundations of China (No. 81703541 and 81673322). This work was supported by MEDCHEMEXPRESS. Thanks to MCE Award for Scientists Promoting Biology and Medicine Research.

Declaration of interest

The authors declare that there is no conflict of interest regarding the publication of this paper.

References

[1] A.E. Prota, K. Bargsten, D. Zurwerra, J.J. Field, J.F. Díaz, K.-H. Altmann, M.O. Steinmetz, Molecular Mechanism of Action of Microtubule-Stabilizing Anticancer Agents, Science, 339 (2013) 587.

[2] R. Romagnoli, M. Kimatrai Salvador, S. Schiaffino Ortega, P.G. Baraldi, P. Oliva, S. Baraldi, L.C. Lopez-Cara, A. Brancale, S. Ferla, E. Hamel, J. Balzarini, S. Liekens, E. Mattiuzzo, G. Basso, G. Viola, 2-Alkoxycarbonyl-3-arylamino-5-substituted thiophenes as a novel class of antimicrotubule agents: Design, synthesis, cell growth and tubulin polymerization inhibition, Eur. J. Med. Chem., 143 (2018) 683-698.

[3] J. Yang, S. Yang, S. Zhou, D. Lu, L. Ji, Z. Li, S. Yu, X. Meng, Synthesis, anti-cancer evaluation of benzenesulfonamide derivatives as potent tubulin-targeting agents, Eur. J. Med. Chem., 122 (2016) 488-496.

[4] T. Naret, J. Bignon, G. Bernadat, M. Benchekroun, H. Levaique, C. Lenoir, J. Dubois, A. Pruvost, F. Saller, D. Borgel, B. Manoury, V. Leblais, R. Darrigrand, S. Apcher, J.-D. Brion, E. Schmitt, F.R. Leroux, M. Alami, A. Hamze, A fluorine scan of a tubulin polymerization inhibitor isocombretastatin A-4: Design, synthesis, molecular modelling, and biological evaluation, Eur. J. Med. Chem., 143 (2018) 473-490.

[5] R. Kaur, G. Kaur, R.K. Gill, R. Soni, J. Bariwal, Recent developments in tubulin polymerization inhibitors: An overview, Eur. J. Med. Chem., 87 (2014) 89-124.

[6] S. Banerjee, K.E. Arnst, Y. Wang, G. Kumar, S. Deng, L. Yang, G.-b. Li, J. Yang, S.W. White, W. Li, D.D. Miller, Heterocyclic-Fused Pyrimidines as Novel Tubulin Polymerization Inhibitors Targeting the Colchicine Binding Site: Structural Basis and Antitumor Efficacy, J. Med. Chem., 61 (2018) 1704-1718.

[7] A.A. Ghawanmeh, K.F. Chong, S.M. Sarkar, M.A. Bakar, R. Othaman, R.M. Khalid, Colchicine prodrugs and codrugs: Chemistry and bioactivities, Eur. J. Med. Chem., 144 (2018) 229-242.

[8] G.F. Mangiatordi, D. Trisciuzzi, D. Alberga, N. Denora, R.M. Iacobazzi, D. Gadaleta, M. Catto, O. Nicolotti, Novel chemotypes targeting tubulin at the colchicine binding site and unbiasing P-glycoprotein, Eur. J. Med. Chem., 139 (2017) 792-803.

[9] A. Ghinet, A. Tourteau, B. Rigo, V. Stocker, M. Leman, A. Farce, J. Dubois, P. Gautret, Synthesis and biological evaluation of fluoro analogues of antimitotic phenstatin, Bioorg. Med. Chem., 21 (2013) 2932-2940.

[10] A.S. Negi, Y. Gautam, S. Alam, D. Chanda, S. Luqman, J. Sarkar, F. Khan, R. Konwar, Natural

antitubulin agents: Importance of 3,4,5-trimethoxyphenyl fragment, Bioorg. Med. Chem., 23 (2015) 373-389.

[11] S. Ke, L. Shi, X. Cao, Q. Yang, Y. Liang, Z. Yang, Heterocycle-functional gramine analogues: Solvent- and catalyst-free synthesis and their inhibition activities against cell proliferation, Eur. J. Med. Chem., 54 (2012) 248-254.

[12] V. Rachakonda, M. Alla, S.S. Kotipalli, R. Ummani, Design, diversity-oriented synthesis and structure activity relationship studies of quinolinyl heterocycles as antimycobacterial agents, Eur. J. Med. Chem., 70 (2013) 536-547.

[13] H. Mirzaei, S. Emami, Recent advances of cytotoxic chalconoids targeting tubulin polymerization: Synthesis and biological activity, Eur. J. Med. Chem., 121 (2016) 610-639.

[14] B. Dasari, R. Jimmidi, P. Arya, Selected hybrid natural products as tubulin modulators, Eur. J. Med. Chem., 94 (2015) 497-508.

[15] D.J. Fu, L. Fu, Y.C. Liu, J.W. Wang, Y.Q. Wang, B.K. Han, X.R. Li, C. Zhang, F. Li, J. Song, Structure-Activity Relationship Studies of β-Lactam-azide Analogues as Orally Active Antitumor Agents Targeting the Tubulin Colchicine Site, Sci Rep., 7 (2017) 12788.

[16] Fu, Dongjun, Liu, Yingchao, Li, Feng, Zhang, En, Liu, Hongmin, Recent Advances in Asymmetric Synthesis of Oxacephems, Chin. J.Org. Chem., 35 (2015) 947.

[17] D.J. Fu, J.F. Liu, R.H. Zhao, J.H. Li, S.Y. Zhang, Y.B. Zhang, Design and Antiproliferative Evaluation of Novel Sulfanilamide Derivatives as Potential Tubulin Polymerization Inhibitors, Molecules, 22 (2017) 1470.

[18] D.J. Fu, S.Y. Zhang, Y.C. Liu, L. Zhang, J.J. Liu, J. Song, R.H. Zhao, F. Li, H.H. Sun, H.M. Liu, Design, synthesis and antiproliferative activity studies of novel dithiocarbamate-chalcone derivates, Bioorg. Med. Chem. Lett., 26 (2016) 3918.

[19] D.J. Fu, L. Zhang, J. Song, R.W. Mao, R.H. Zhao, Y.C. Liu, Y.H. Hou, J.H. Li, J.J. Yang, C.Y. Jin, Design and synthesis of formononetin-dithiocarbamate hybrids that inhibit growth and migration of PC-3cells via MAPK/Wnt signaling pathways, Eur. J. Med. Chem., 127 (2016) 87-99.

[20] D.J. Fu, J. Song, Y.H. Hou, R.H. Zhao, J.H. Li, R.W. Mao, J.J. Yang, P. Li, X.L. Zi, Z.H. Li, Discovery of 5,6-diaryl-1,2,4-triazines hybrids as potential apoptosis inducers, Eur. J. Med. Chem., 138 (2017) 1076-1088.

[21] D.J. Fu, Y.C. Liu, J.J. Yang, J. Zhang, C.D. Xiong, Z.S. Cao, X.X. Yin, W. Wei, Y.B. Zhang, Design and synthesis of sulfonamide-1,2,3-triazole derivatives bearing a dithiocarbamate moiety as antiproliferative agents, J. Chem. Res., (2017).

[22] H.M. Liu, Y.B. Zhang, Y.C. Liu, R.H. Zhao, J. Song, D.J. Fu, Synthesis of novel antiproliferative 1,2,3-triazole hybrids using the molecular hybridisation approach, J. Chem. Res., 40 (2016) -.

[23] D.J. Fu, Y.H. Hou, S.Y. Zhang, Y.B. Zhang, Efficient click reaction towards novel sulfonamide hybrids by molecular hybridization strategy as antiproliferative agents, J. Chem. Sci., 130 (2018) 6.

[24] D.-J. Fu, S.-Y. Zhang, Y.-C. Liu, X.-X. Yue, J.-J. Liu, J. Song, R.-H. Zhao, F. Li, H.-H. Sun, Y.-B. Zhang, H.-M. Liu, Design, synthesis and antiproliferative activity studies of 1,2,3-triazole-chalcones, MedChemComm, 7 (2016) 1664-1671.

[25] D.J. Fu, R.H. Zhao, J.H. Li, J.J. Yang, R.W. Mao, B.W. Wu, P. Li, X.L. Zi, Q.Q. Zhang, H.J. Cai, Molecular diversity of phenothiazines: design and synthesis of phenothiazine-dithiocarbamate hybrids as potential cell cycle blockers, Mol. Diver., (2017) 1-10.

[26] Y.B. Zhang, H.M. Liu, X.L. Zi, R.H. Zhao, L. Zhang, Y.C. Liu, J. Song, S.Y. Zhang, D.J. Fu, Design and antiproliferative activity of N-heterocycle-chalcone derivatives, J. Chem. Res., 40 (2016) -.

[27] Y.B. Zhang, H.M. Liu, R.W. Mao, R.H. Zhao, J. Song, Y.C. Liu, S.Y. Zhang, D.J. Fu, Design, synthesis and antiproliferative evaluation of 3-aminopropyloxy derivatives of chalcone, J. Chem. Res., 40 (2016) -.

[28] K.R. Senwar, T.S. Reddy, D. Thummuri, P. Sharma, V.G.M. Naidu, G. Srinivasulu, N. Shankaraiah, Design, synthesis and apoptosis inducing effect of novel (Z)-3-(3′-methoxy-4′-(2-amino-2-oxoethoxy)-benzylidene)indolin-2-ones as potential antitumour agents, Eur. J. Med. Chem., 118 (2016) 34-46.

[29] A. Strasser, S. Cory, J.M. Adams, Deciphering the rules of programmed cell death to improve therapy of cancer and other diseases, The EMBO Journal, 30 (2011) 3667-3683.

[30] P.E. Czabotar, G. Lessene, A. Strasser, J.M. Adams, Control of apoptosis by the BCL-2 protein family: implications for physiology and therapy, Nat. Rev. Mol. Cell Bio., 15 (2013) 49.

[31] A. Abou Samra, A. Robert, C. Gov, L. Favre, L. Eloy, E. Jacquet, J. Bignon, J. Wiels, S. Desrat, F. Roussi, Dual inhibitors of the pro-survival proteins Bcl-2 and Mcl-1 derived from natural compound meiogynin A, Eur. J. Med. Chem., 148 (2018) 26-38.

[32] O. Gavet, J. Pines, Progressive Activation of CyclinB1-Cdk1 Coordinates Entry to Mitosis, Dev. Cell, 18 (2010) 533-543.

[33] L.T. Vassilev, C. Tovar, S. Chen, D. Knezevic, X. Zhao, H. Sun, D.C. Heimbrook, L. Chen, Selective small-molecule inhibitor reveals critical mitotic functions of human CDK1, Proc. Nati. Acad. Sci., 103 (2006) 10660-10665.

[34] M. Juhaszova, D.B. Zorov, S.-H. Kim, S. Pepe, Q. Fu, K.W. Fishbein, B.D. Ziman, S. Wang, K. Ytrehus, C.L. Antos, E.N. Olson, S.J. Sollott, Glycogen synthase kinase-3β mediates convergence of protection signaling to inhibit the mitochondrial permeability transition pore, J. Clin. Invest., 113 (2004) 1535-1549.

[35] D.J. Fu, L. Fu, Y.C. Liu, J.W. Wang, Y.Q. Wang, B.K. Han, X.R. Li, C. Zhang, F. Li, J. Song, Structure-Activity Relationship Studies of β -Lactam-azide Analogues as Orally Active Antitumor Agents Targeting the Tubulin Colchicine Site, Sci Rep, 7 (2017) 12788.

Highlights

.4d exhibited the potent antiproliferative activity against MGC-803 cells.

.4d induced cell cycle G2/M phase arrest and apoptosis.

.4d changed the mitochondrial membrane potential against MGC-803 cells.

.4d acted as a novel colchicine site tubulin polymerization inhibitor.